62 63029

[redacted]

Copy 26
RM SL54K19

NACA

RESEARCH MEMORANDUM

for the

U. S. Air Force

EE-FLIGHT INVESTIGATION OF THE FULL-SCALE HUGHES FALCON MISSILE, D CONFIGURATION, TO DETERMINE AILERON EFFECTIVENESS AND DAMPING IN ROLL

By Reginald R. Lundstrom

Langley Aeronautical Laboratory
Langley Field, Va.

[redacted]

NATIONAL ADVISORY COMMITTEE
FOR AERONAUTICS

WASHINGTON

NOV 19 1954

[redacted]

NATIONAL ADVISORY COMMITTEE FOR AERONAUTICS

RESEARCH MEMORANDUM

for the

U. S. Air Force

FREE-FLIGHT INVESTIGATION OF THE FULL-SCALE HUGHES FALCON MISSILE, D CONFIGURATION, TO DETERMINE AILERON EFFECTIVENESS AND DAMPING IN ROLL

By Reginald R. Lundstrom

SUMMARY

A free-flight investigation was conducted over the Mach number range from 0.8 to 1.8 near zero lift to determine the aileron effectiveness and damping in roll of the full-scale Hughes Falcon missile, D configuration. Drag-coefficient data were also determined. Aileron-effectiveness coefficient per degree aileron C_{l_δ} based on body diameter and body cross-sectional area had a peak value of 0.094 at Mach number 0.96 and decreased to a value of 0.037 at the maximum Mach number of the test. The damping-in-roll derivative C_{l_p} based on body diameter and body cross-sectional area had approximately a constant value of 23 over the Mach number range of the test. The drag coefficient based on body cross-sectional area was about 0.4 up to a Mach number of 0.9 and gradually increased to about 0.8 at a Mach number of 1.2 and remained at 0.8 up to the maximum Mach number of the test.

INTRODUCTION

At the request of the U. S. Air Force, the Langley Pilotless Aircraft Research Division is conducting free-flight tests of the full-scale Hughes Falcon missile in an effort to obtain stability and control effectiveness information. Results obtained from rocket model tests of the C configuration of the Hughes Falcon missile to obtain longitudinal stability information may be found in reference 1.

The present report gives results from a flight test conducted to determine aileron effectiveness and damping in roll of the D configuration of the Falcon missile near zero lift over the Mach number range from 0.8 to 1.8 and corresponding Reynolds number range of approximately 4×10^6 to 12×10^6 per foot. The approximately zero-lift drag as obtained from this flight test is also included.

Inasmuch as these tests were conducted at low altitude, the model as furnished by the Hughes Company was made much heavier than the tactical missile in order that the deceleration would be lower over that part of the flight during which the data were obtained. The desired Mach number was obtained by using a booster made up of two solid-fuel ABL Deacon rockets with suitable-size stabilizing fins.

SYMBOLS

d	body diameter, 0.533 ft
q	dynamic pressure, lb/sq ft
g	acceleration due to gravity, 32.2 ft/sec^2
M	Mach number
S	maximum body cross-sectional area, 0.223 sq ft
V	free-stream velocity, ft/sec
W	model weight, 179.5 lb
a_l	model acceleration along flight path, ft/sec^2
γ	model flight-path angle measured from the horizontal, deg
δ	aileron deflection, deg ($\delta = 2^\circ$ means one aileron up 2° and other down 2°; positive δ will cause model to roll clockwise, viewed from rear)
δ_p	positive δ
δ_n	negative δ
I_X	moment of inertia about body longitudinal axis, slug-ft^2

I_Y moment of inertia about Y-axis, slug-ft^2

I_Z moment of inertia about Z-axis, slug-ft^2

C_D drag coefficient, Drag/qS

ϕ body roll angle, radians

$\dot{\phi}$ roll rate, radians/sec

$\ddot{\phi}$ roll acceleration, radians/sec^2

C_l rolling-moment coefficient, $\dfrac{\text{Rolling moment}}{qSd}$

C_{l_o} out-of-trim rolling-moment coefficient

$$C_{l_\delta} = \frac{\partial C_l}{\partial \delta}$$

$$C_{l_p} = \frac{\partial C_l}{\partial \frac{\dot{\phi} d}{2V}}$$

APPARATUS AND METHOD

Model Description and Test

The Hughes Falcon D configuration is a cruciform winged missile with small forward lifting surfaces of low aspect ratio and larger rear lifting surfaces of very low aspect ratio. The aerodynamically balanced flap controls are at the trailing edge of the rear lifting surfaces. The body is cylindrical except for the nose and boattail sections. A sketch of the model is shown in figure 1 and a photograph, in figure 2. Details of the lifting surfaces and controls are shown in figure 3. The body coordinates are listed in table I. The model was constructed from steel except for the nose section which was made of brass for ballast purposes and the rear wings which were made of 24S-T4 aluminum alloy. The control surfaces were made of steel. Physical characteristics of the model are presented in table II.

The ailerons were programmed in a square-wave pattern by means of a hydraulic pulse system, and the control surfaces were against the stops for longer periods of time at the lower Mach numbers in order to allow the roll rate to build up close to the steady-state value during each pulse. About $1/4^{\circ}$ of free play existed in one of the control surfaces. Since unpublished wind-tunnel data show these control surfaces to be aerodynamically underbalanced, it has been assumed that this play would at all times be taken up so as to make the control deflection closer to zero. The measured aileron deflections at the stops were $\delta = -1.87^{\circ}$ and $\delta = 2^{\circ}$.

Instrumentation

The model was equipped with an NACA eight-channel telemeter. Quantities measured were normal, transverse, and longitudinal accelerations, roll rate and acceleration, control position, total head pressure, and body static pressure. A Doppler velocimeter was used to obtain velocity, and tracking radar was used to obtain the position of the model as a function of flight time. Atmospheric conditions at the time of flight were obtained from a radiosonde.

Reduction of Data

Reduction of data was made using the single-degree-of-freedom roll equation:

$$\frac{I_X\ddot{\phi}}{qSd} - C_{l_p}\left(\frac{d}{2V}\right)\dot{\phi} = -\left(C_{l_\delta}\delta + C_{l_o}\right)$$

Since the quantity C_{l_p} desired was the roll-damping derivative of the entire configuration rather than the particular wing plan form, no effort was made to account for interference effects. As the controls were pulsed between approximately 2° and -2°, at some time during each pulse, $\dot{\phi} = 0$. When $\dot{\phi} = 0$, $\left(C_{l_\delta}\delta + C_{l_o}\right) = -\frac{I_X\ddot{\phi}}{qSd}$ and $\left(C_{l_\delta}\delta + C_{l_o}\right)$ was plotted as a function of Mach number for both the positive and negative control deflections. A curve was faired through the points obtained from the positive control deflection and another through the points of negative control deflection. The difference between these curves is as follows:

$$\left(C_{l_\delta}\delta_p + C_{l_o}\right) - \left(C_{l_\delta}\delta_n + C_{l_o}\right) = C_{l_\delta}\delta_p - C_{l_\delta}\delta_n = C_{l_\delta}\left(\delta_p - \delta_n\right)$$

This equation divided by $\left(\delta_p - \delta_n\right)$ gave the desired quantity C_{l_δ}. With $\left(C_{l_\delta}\delta + C_{l_o}\right)$ known as a function of Mach number, C_{l_p} then became the only unknown in the roll equation and could be determined. Greatest accuracy in determining C_{l_p} could be obtained by substituting values of $\ddot{\phi}$ and $\dot{\phi}$ near the end of each pulse when $\ddot{\phi}$ was closest to its steady-state value.

Drag data were reduced from the relationship $C_D = -\dfrac{W\left(a_l + g \sin \gamma\right)}{gqS}$. The acceleration a_l was determined by differentiation of the velocity-time curve obtained from the Doppler radar because the longitudinal accelerometer did not operate properly.

Accuracy

The point accuracy of the quantities listed is believed to be within the following limits:

C_{l_δ} . . . . ±5 percent
C_{l_p} . . . . ±10 percent
C_D . . . . ±3 percent
V . . . . ±1 percent
M . . . . ±1 percent

RESULTS AND DISCUSSION

The Reynolds number per foot for these tests varied from 3.85×10^6 at $M = 0.8$ to 12.15×10^6 at $M = 1.8$. Some transient pitching and yawing motion resulted from the abrupt change in aileron position. The angle of attack or sideslip in almost all cases was determined to be less than 1° and the peaks of the normal and lateral oscillations about 90° out of phase. A sample time history of $\dot{\phi}$, $\ddot{\phi}$, and δ as the model coasted through the Mach number range is presented in figure 4. Because of the relatively slow response of the instrument measuring roll acceleration, it was necessary to apply a time-lag correction to the values of roll acceleration used in reducing the data. The corrected roll-acceleration values were in very good agreement with values obtained by differentiating the roll rate. In figure 4 no attempt was made to correct the roll acceleration during or immediately after the time the control surfaces moved from one position to the other. It may be noted that $\ddot{\phi}$ did not pass through zero during the first pulse because the out-of-trim moment was in the same direction as the pulse. Values of $\left(C_{l_\delta}\delta + C_{l_o}\right)$ and C_{l_p} were reduced from this pulse by using a method of least squares. The rolling-moment coefficients for the other pulses were obtained by using the value of $\ddot{\phi}$ when $\dot{\phi} = 0$ mentioned under the section "Reduction of Data." Variation of rolling-moment coefficient with Mach number is shown in figure 5. The rolling-moment coefficient is plotted positive for both positive and negative δ to show the change in out-of-trim moment with Mach number. Aileron effectiveness, C_{l_δ}, as obtained from rolling-moment coefficient is presented as a function of Mach number in figure 6. The trend of C_{l_δ} against M corresponds closely to the flap lift effectiveness shown in reference 2 and if the spanwise center of pressure of the flap is assumed to be at the center of exposed span of the flap, the order of magnitude is also the same.

The damping-in-roll derivative C_{l_p} is presented as a function of Mach number in figure 7. The values of C_{l_p} shown are for roll rates of about 20 radians per second. An attempt was made to determine the variation of C_{l_p} with $\dot{\phi}$. Although it was in general indicated that C_{l_p} was 5 to 10 percent lower at 10 radians per second than at 20 radians per second, this was not always the case and because this is within the probable accuracy band, the results are not presented. It will be noted that C_{l_p} is practically independent of Mach number. Direct comparison with theory is impractical for this configuration because of the large radius at the leading edge of the rearward surface body juncture and the effects of interference from the forward surface. Theory, however (for example, see refs. 3 and 4), does indicate the general order of magnitude and the fact that for such a low aspect ratio, C_{l_p} is practically independent of Mach number. Reference 5 which gives experimental data on delta wings with leading-edge sweep up to 70° also checks this order of magnitude and trend.

Variation of drag coefficient with Mach number is presented in figure 8. The drag coefficient was about 0.4 up to a Mach number of 0.9, and gradually increased to 0.8 at a Mach number of 1.2 and remained at 0.8

up to the maximum Mach number of the test. This is in very close agreement with unpublished flight-test data obtained from Hughes Aircraft Company. The drag-coefficient curve has the same general shape as that of the Falcon C configuration shown in reference 1; however, the fact that the C configuration model had an angle-of-attack vane in front of the blunt nose which may have affected the drag precludes any possibility for direct comparison of magnitude of drag coefficient.

CONCLUSIONS

A rocket-model test of the full-scale Hughes Falcon missile, D configuration, over a Mach number range from 0.8 to 1.8 gave the following results (coefficients based on body diameter and cross-sectional area):

(1) The rolling-moment coefficient per degree aileron increased to a maximum value of 0.094 at Mach number 0.96 and decreased to a value of 0.037 at the maximum Mach number of the test. The trend with Mach number was much the same as the trend of normal-force coefficient per degree elevator for a similar trailing-edge flap on a 60° delta wing. When the normal-force coefficients are converted to rolling-moment coefficients, the order of magnitude is also the same.

(2) The damping-in-roll derivative C_{l_p} was approximately constant at a value of 23 over the Mach number range tested. This trend and order of magnitude is indicated by theory and flight tests on delta wings.

(3) The drag coefficient based on body cross-sectional area was about 0.4 up to a Mach number of 0.9 and gradually increased to about 0.8 at a Mach number of 1.2 and remained at 0.8 up to the maximum Mach number of the test.

Langley Aeronautical Laboratory,
National Advisory Committee for Aeronautics,
Langley Field, Va., November 3, 1954.

Reginald R. Lundstrom

Reginald R. Lundstrom
Aeronautical Research Scientist

Approved: Joseph A. Shortal

Joseph A. Shortal
Chief of Pilotless Aircraft Research Division

rwh

[redacted]

REFERENCES

1. Baber, Hal T., Jr. and Moul, Martin T.: Longitudinal Stability and Control Characteristics of the "C" Configuration of the Hughes Falcon Missile for a Range of Mach Number From 0.7 to 1.8 as Determined From Flight Test of a Ground-Launched Model. NACA RM SL54B12, U. S. Air Force, 1954.

2. Martz, C. William, and Goslee, John W.: Rocket-Model Investigation To Determine the Hinge-Moment and Normal-Force Properties of a Full-Span, Constant-Chord Partially Balanced Trailing-Edge Control on a 60° Clipped Delta Wing Between Mach Numbers of 0.50 and 1.26. NACA RM L53I04, 1953.

3. Piland, Robert O.: Summary of the Theoretical Lift, Damping-in-Roll, and Center-of-Pressure Characteristics of Various Wing Plan Forms at Supersonic Speeds. NACA TN 1977, 1949.

4. Miles, John W.: On the Damping in Roll of a Slender Cruciform Winged Body. NAVORD Rep. 2043 (NOTS 732), U. S. Naval Ord. Test Station (Inyokern, Calif.), July 16, 1953.

5. Sanders, E. Claude, Jr.: Damping in Roll of Models with 45°, 60°, and 70° Delta Wings Determined at High Subsonic, Transonic, and Supersonic Speeds With Rocket-Powered Models. NACA RM L52D22a, 1952.

TABLE I

BODY CONTOUR ORDINATES OF MODEL TESTED

[All dimensions in inches]

Station	Radius	Station	Radius
8.658	0	11.808	2.690
8.758	.663	11.908	2.708
8.858	.927	12.008	2.724
8.958	1.122	12.108	2.739
9.058	1.281	12.208	2.753
9.158	1.414	12.308	2.765
9.258	1.530	12.353	2.771
9.317	1.591	12.453	2.782
9.408	1.677	12.553	2.792
9.508	1.762	12.653	2.802
9.608	1.840	12.753	2.812
9.708	1.911	12.853	2.821
9.808	1.976	13.042	2.837
9.908	2.037	14.604	2.958
10.008	2.093	15.832	3.034
10.108	2.146	17.442	3.110
10.208	2.196	18.506	3.147
10.308	2.242	19.642	3.175
10.408	2.286	20.495	3.190
10.508	2.327	21.179	3.197
10.608	2.366	21.842	3.200
10.708	2.403	23.00	3.200
10.808	2.437	80.00	3.200
10.908	2.470	81.00	3.200
11.008	2.501	81.50	3.193
11.108	2.530	82.00	3.173
11.208	2.557	82.50	3.143
11.308	2.583	83.00	3.106
11.408	2.607	83.50	3.064
11.508	2.630	84.00	3.019
11.608	2.651	86.5	2.793
11.708	2.671		

TABLE II

PHYSICAL CHARACTERISTICS OF MODEL TESTED

Weight, lb	179.5
Center-of-gravity station	51.44
I_X, slug-ft^2	0.43
I_Y, slug-ft^2	18.71
I_Z, slug-ft^2	18.71
Body diameter (cylindrical section), ft	0.533
Body cross-sectional area, sq ft	0.223
Total wing area per plane forward surface, (total wing area of forward surface includes the fuselage profile area between station 13.70 and 21.40), sq ft	0.446
Total wing area per plane rearward surface including control, (total wing area of rearward surface includes the fuselage profile area between station 42.50 and 81.95), sq ft	4.129
Exposed area of two control surfaces, sq ft	0.301

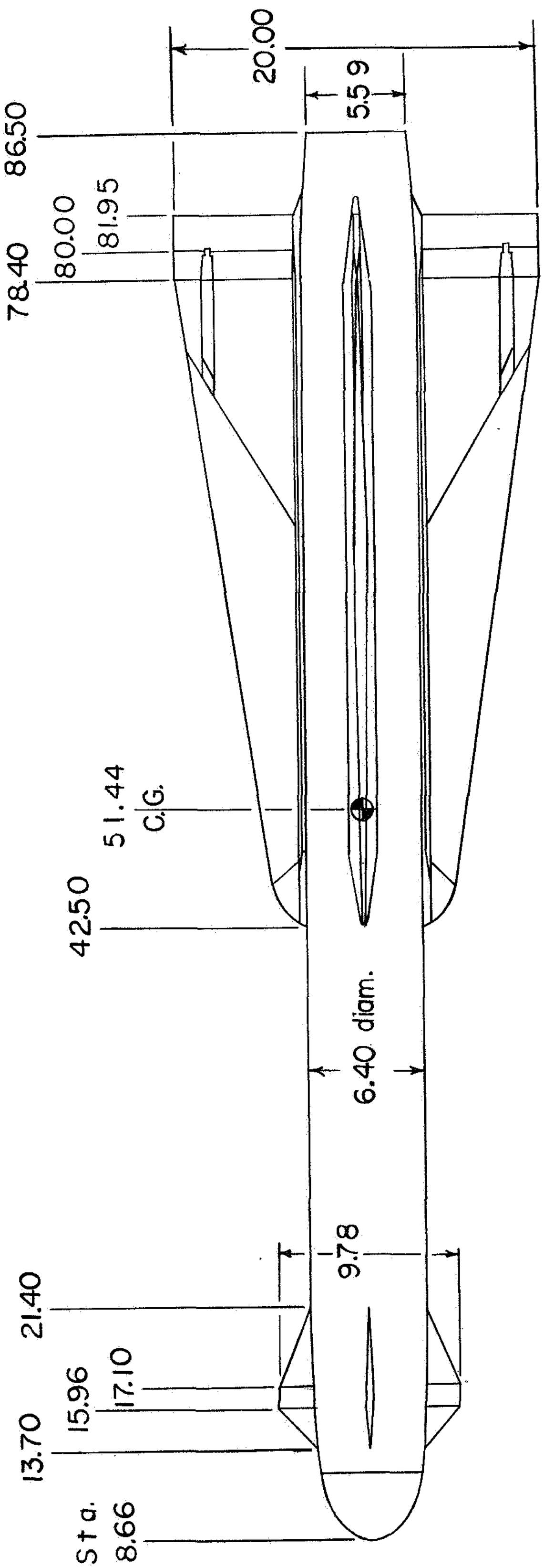

Figure 1.- General model arrangement. All dimensions in inches.

[redacted]

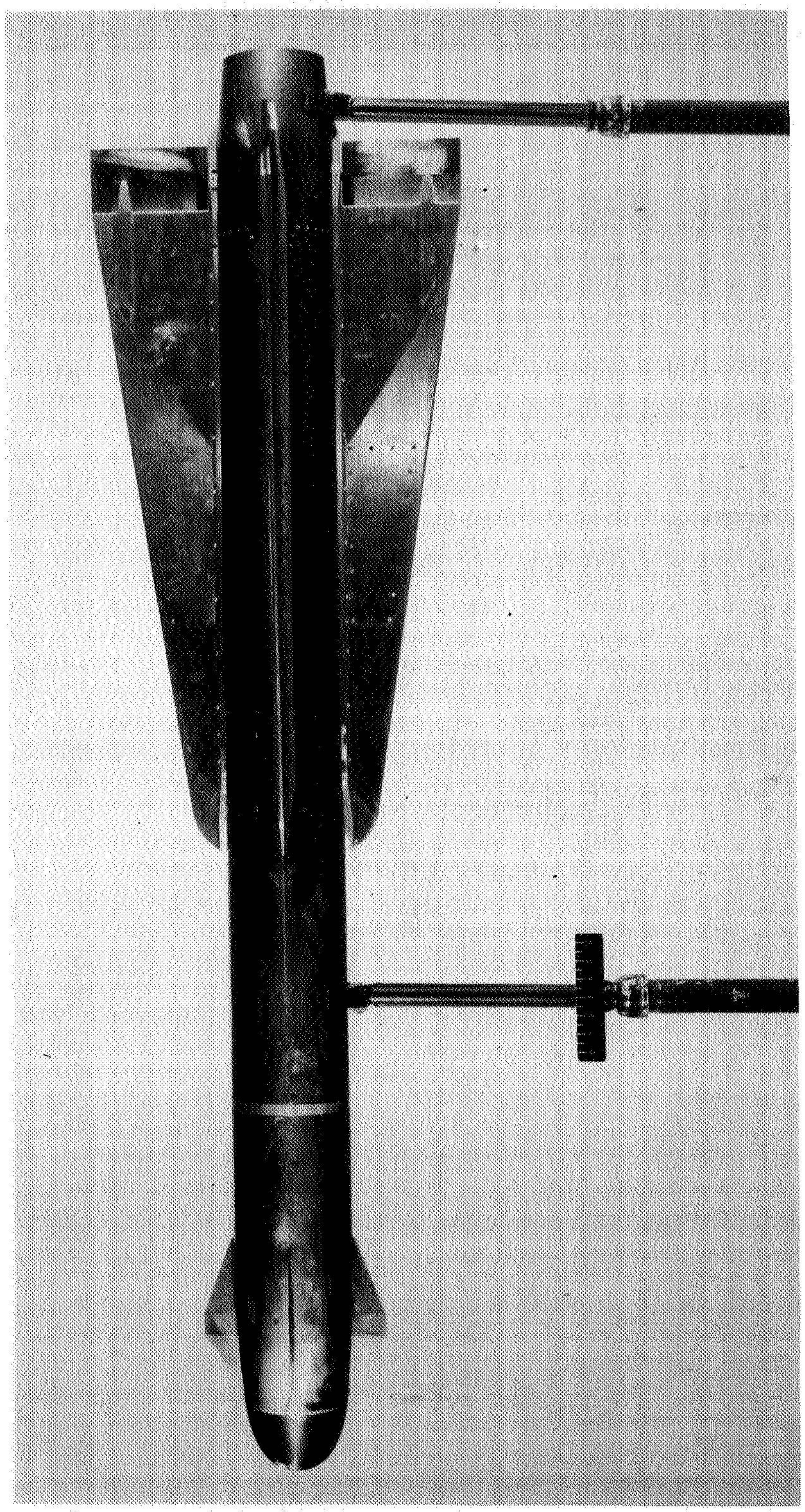

L-81365.1

Figure 2.- Model tested.

[redacted]

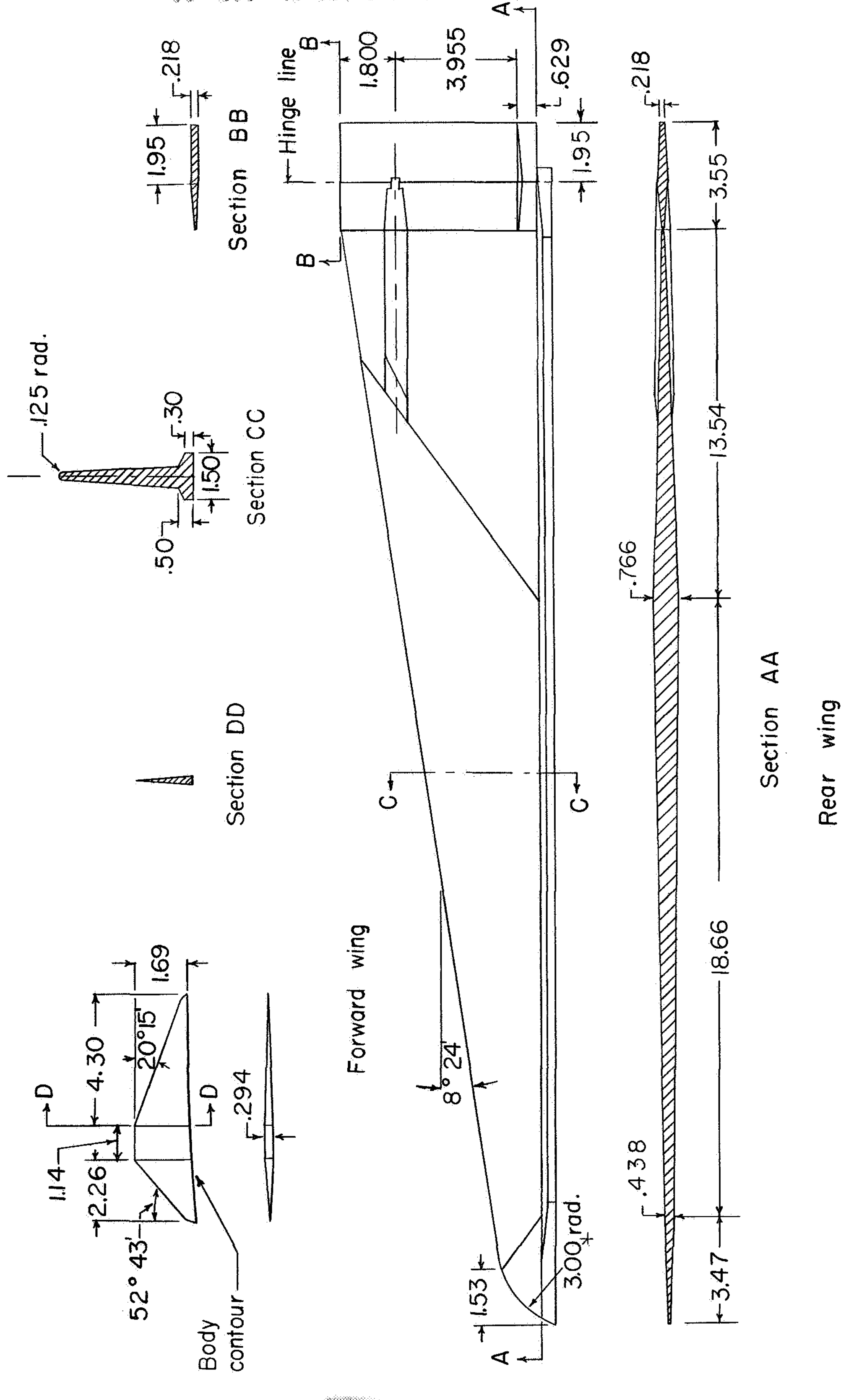

Figure 3.- Lifting-surface details.

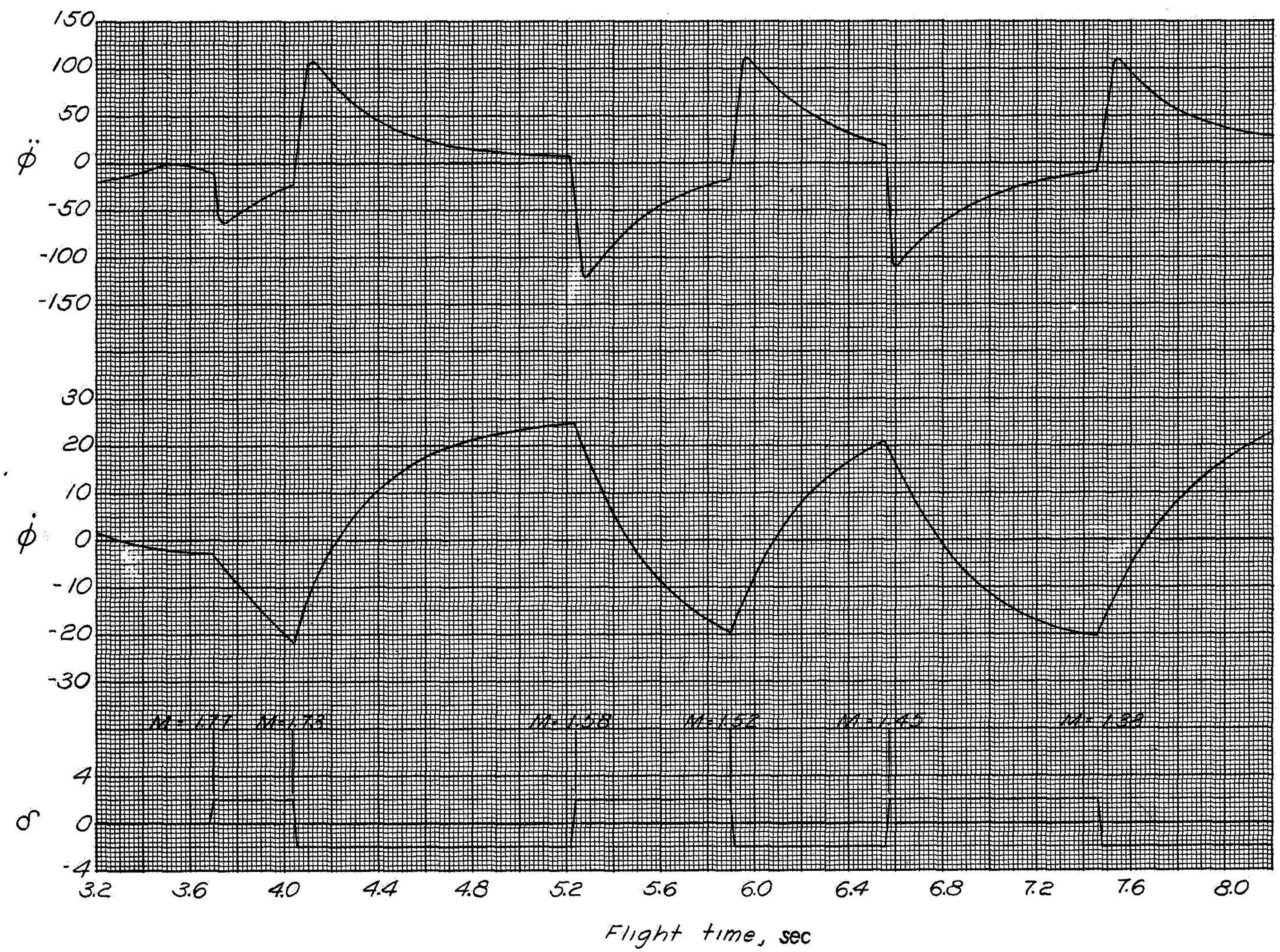

Figure 4.- Sample time history of aileron position, roll rate, and roll acceleration.

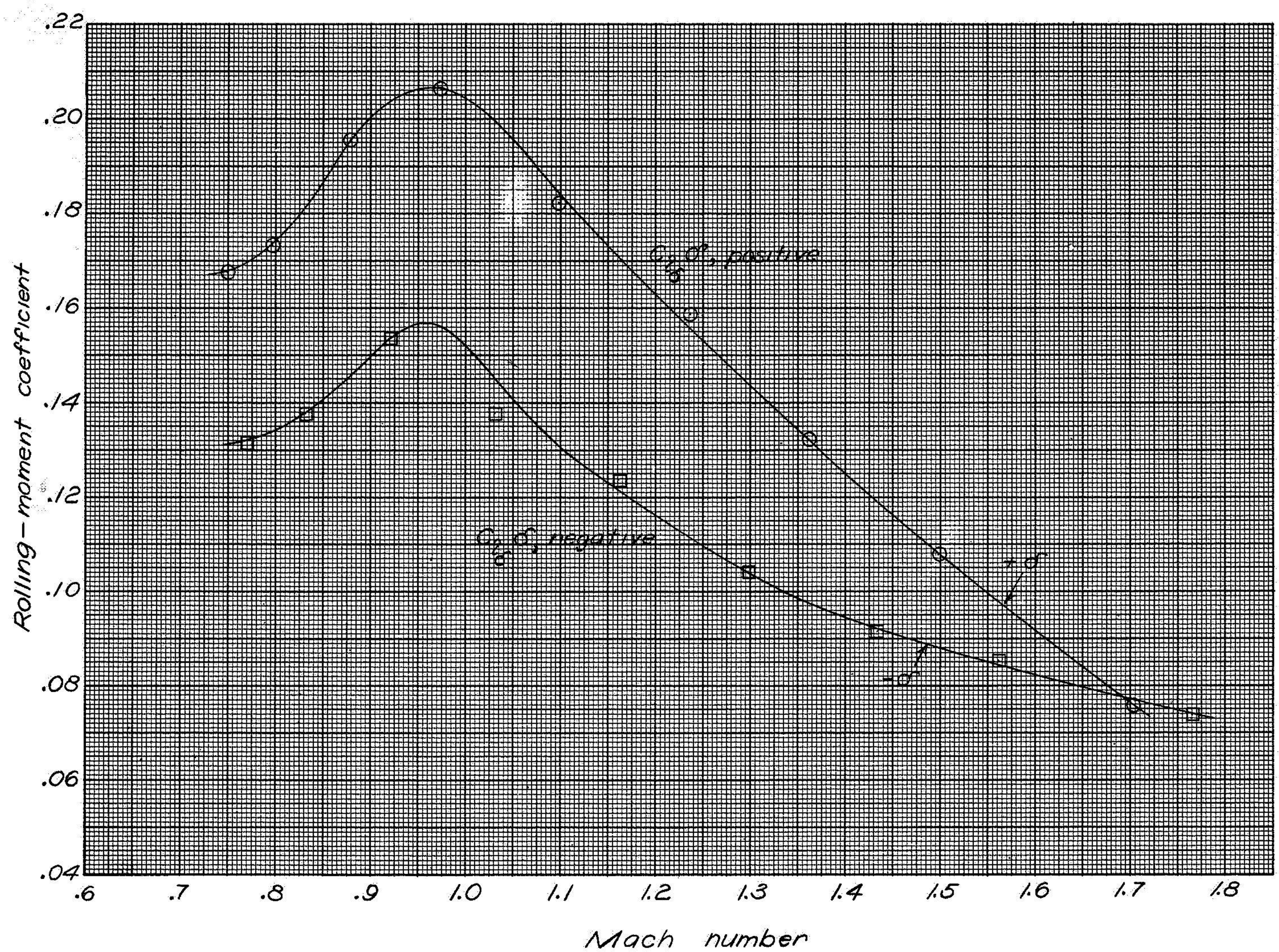

Figure 5.- Rolling-moment coefficient as a function of Mach number for positive and negative aileron deflections.

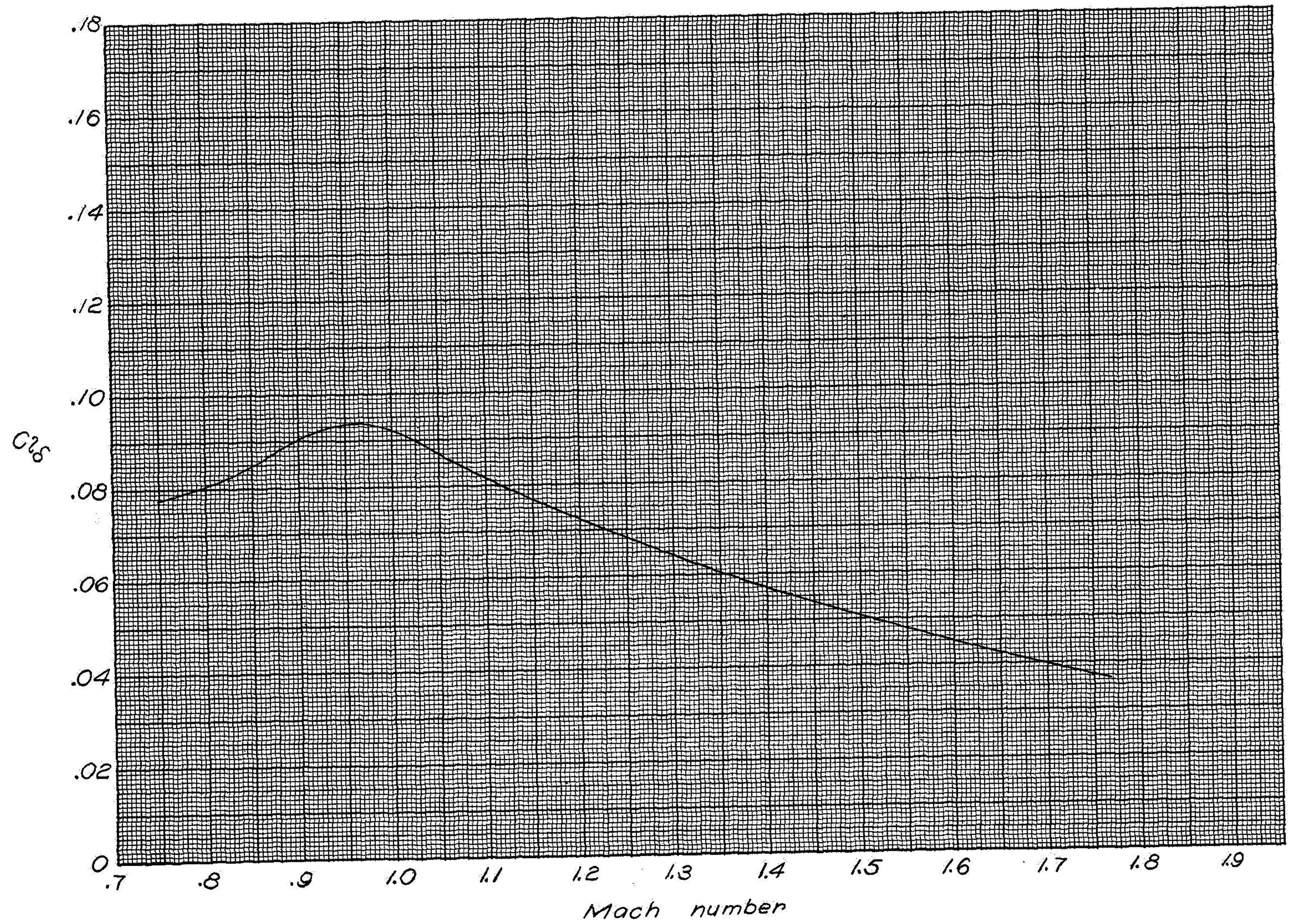

Figure 6.- Variation of C_{l_δ} with Mach number.

[redacted]

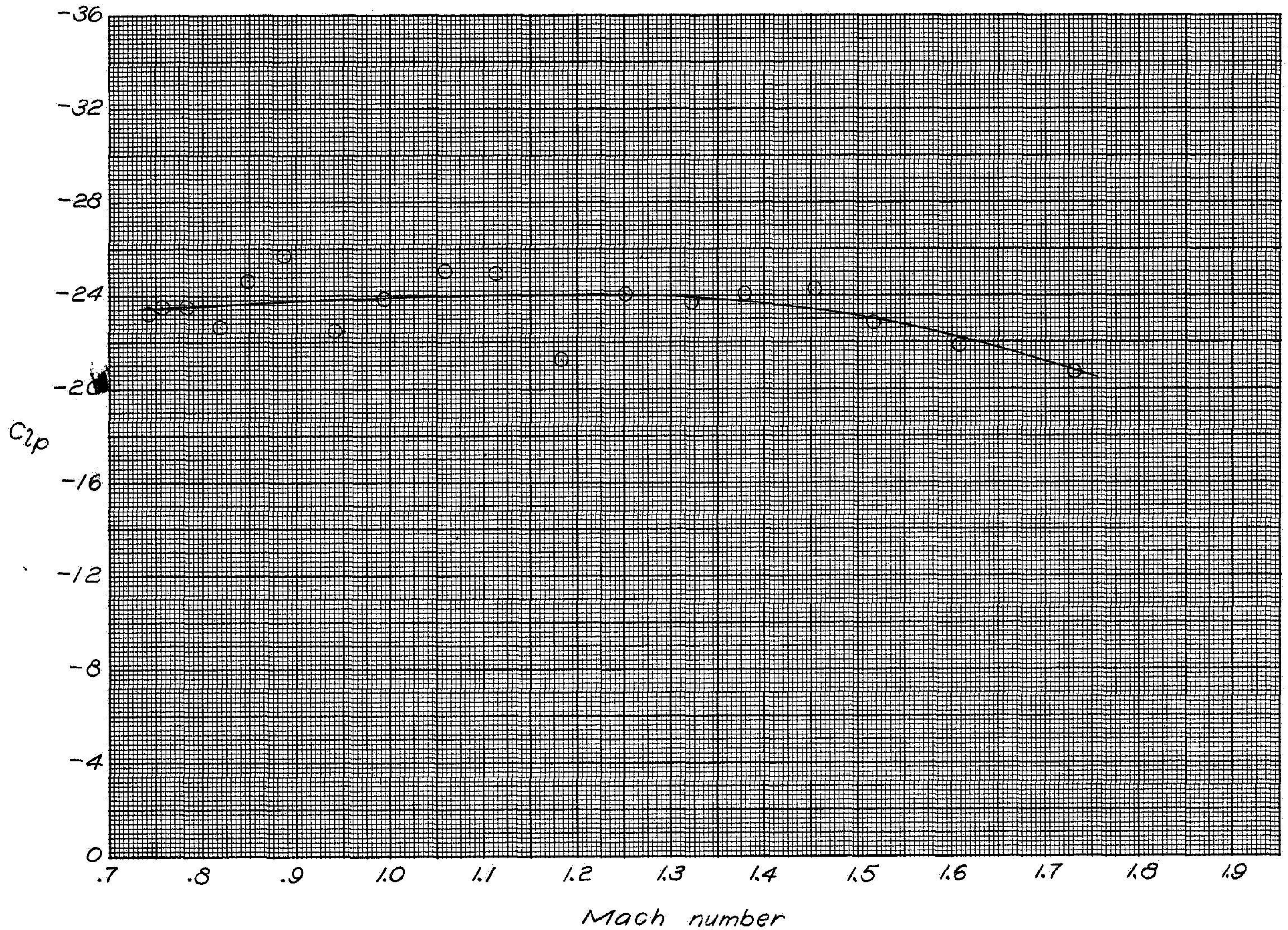

Figure 7.- Variation of C_{l_p} with Mach number.

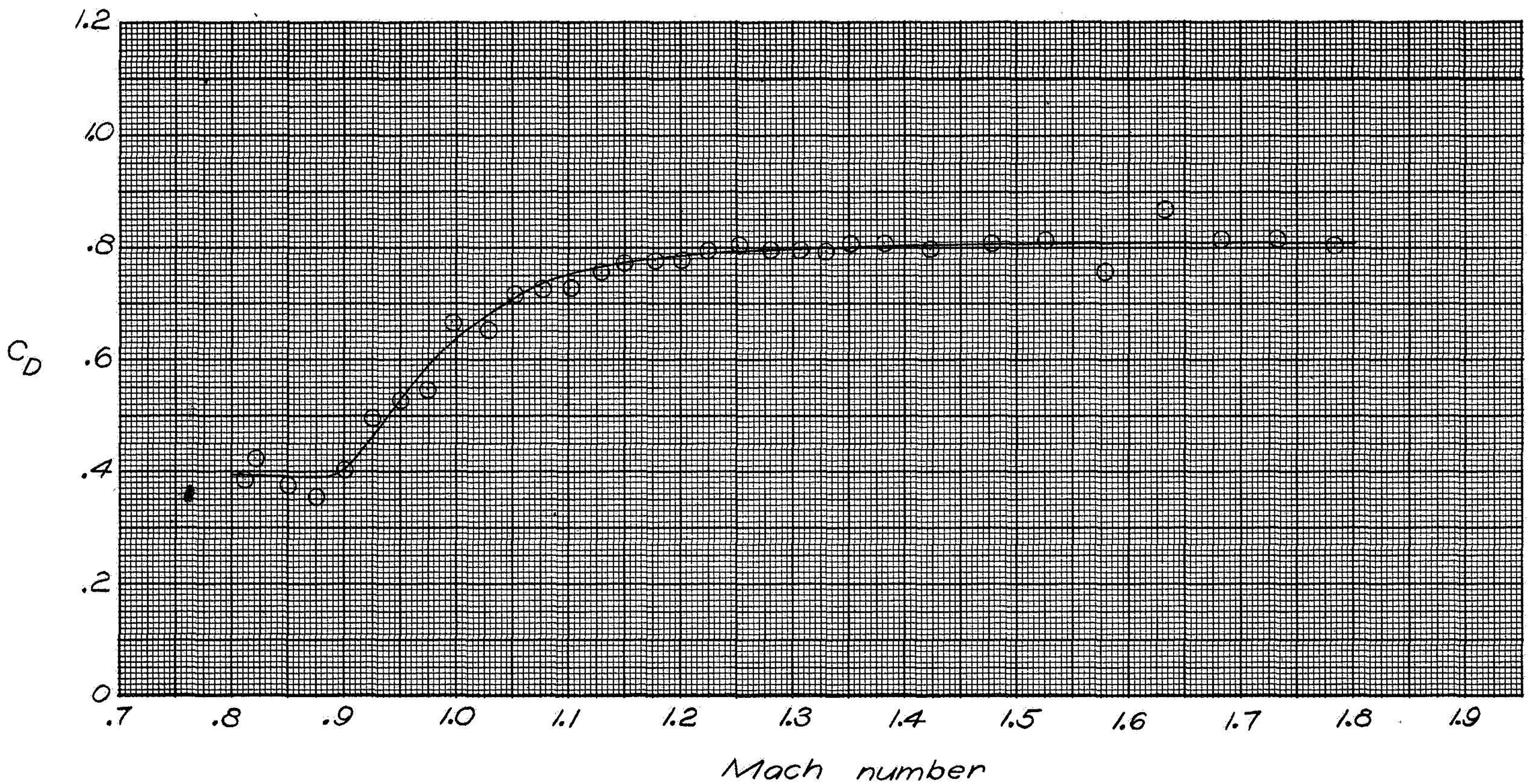

Figure 8.- Variation of C_D with Mach number.

[redacted]

SERVICE REPORT

[redacted]